CHAPTER 3 METHODOLOGY

In order to achieve the objectives of this study, a series of physical model test on flexible pavement structure applied with cyclic loads were carried out. The pavement structures were modeled from full-scale pavement to small-scale model in laboratory. The subbase layer in laboratory was modified and replaced by cleaned sand (KMUTT sand). The polymer modified asphaltic concrete and geosynthetics were placed on the top of subbase. Both new pavements and overlay pavements were studied. All the tests were performed in a temperature controlled laboratory (≈ 25 ^{o}C).

3.1 Physical Model Test

3.1.1 Small-scale experimental

In this study, a small-scale model structure was used to model flexible pavement structure in laboratory. The approach of scaled-down modeling was chosen because (Jumikis, 1963):

1. It is easier to handle the testing apparatus than a full-scale prototype
2. Small-scale studies are less expensive than full-scale ones
3. It is possible to eliminate many factors involved, and to control and observe only those in which one is particularly interested
4. By artificially simulating field conditions in the laboratory it is possible to
    a.) Observe conveniently the rupture process and shapes of deformation in prototype soil, and
    b.) Perform actual measurements of deformations in the model soil under given loading conditions, thus obtaining the data for the correlation of pertinent facts
    c.) Model the prototype system
5. The researcher, in performing stability calculations of prototype soil-foundation-load systems, is released from making several assumptions usually made in the mathematical approach

3.1.2 Model of wheel load

Figure 3.1 and Figure 3.2 show wheel load simulation employed in this study. A load, which was transferred to footing model, was simulated from a standard wheel load of 18 kips (AASHTO, 1993). Therefore, each wheel is loaded at 4.5 kips (4,500 lb). Then, the standard wheel load was converted to a standard single wheel load (ESWL, P_s) by stress factors principle (Equation 3.1 and Figure 3.3), which was proposed by Boussinesq (1885).

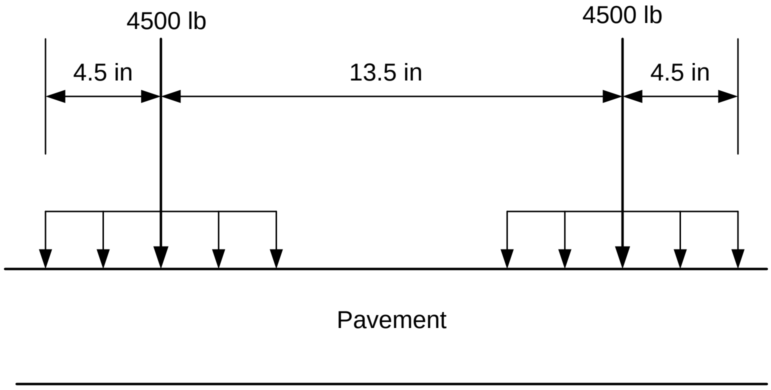

Figure 3.1 Distribution of wheel load in this study

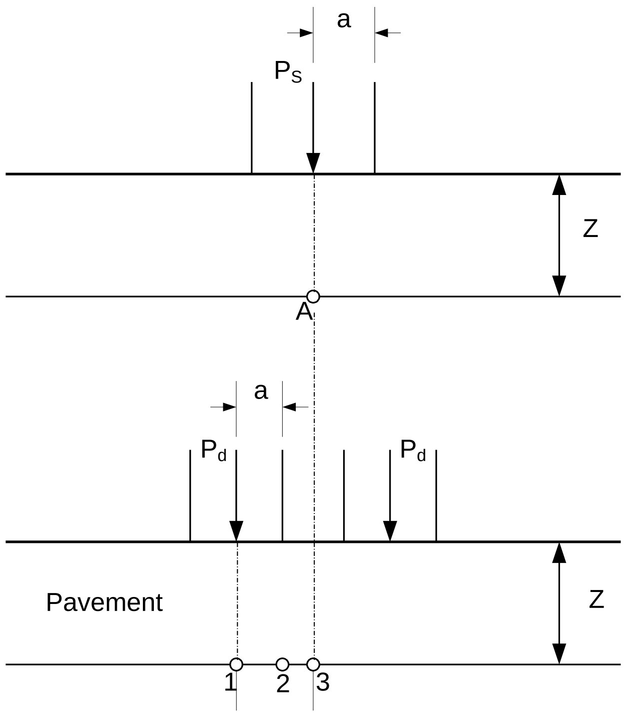

Figure 3.2 Conversion of wheel load to standard single wheel

$$\frac{P_s}{P_d} = \frac{\sigma_z / q_d}{\sigma_z / q_s} \tag{3.1}$$

where; P_s = Equivalent single wheel load (ESWL)

P_d = Load from each wheel

σ_z = vertical stress

q_d, q_s = pressure under P_d, P_s

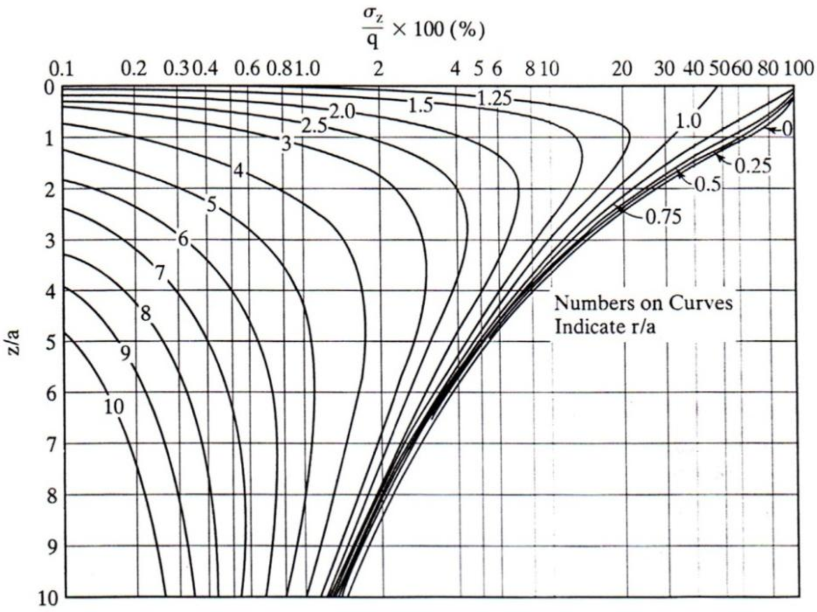

Figure 3.3 Relationship between depth and stress factor (Huang, 2004)

From Equation 3.1 and Figure 3.3, the stress factor calculation was considered at 13.5 inch depth from pavement surface. The stress factor for point nos. 1, 2, and 3 (Figure. 3.4) are shown in Table 3.1.

Table 3.1 Relationship between stress factor and depth/a radius of wheel

Point no.	Left wheel		Right wheel		Sum
	r/a	σ_z/q_s	r/a	σ_z/q_s	σ_z/q_d
1	0	0.143	3	0.03	0.173
2	0.75	0.126	2.25	0.053	0.179
3	1.5	0.088	1.5	0.088	0.176

From Table 3.1, the stress factor at A and 2 (Figure 3.2) is equal 0.143 and 0.179 respectively. Thus, the ESWL (P_s) is calculated by Equation 3.1.

$$P_s = \frac{\sigma_z/q_d}{\sigma_z/q_s} P_d = \frac{0.179}{0.143} \times 4500 = 5630\,lb. \approx 25.1\,kN$$

Then, the result of above equation was used in calculated a stress which transfers to the model footing having dimension of 6x40 cm. It is equal 1,045.8 kPa. According to the small-scale modeling, stress was used about 40% from the actual stress in the full-scale case. Therefore, the maximum stress during cyclic loading, which was used in this study, is equal 400 kPa.

3.2 Materials

The pavement structures modeled from full-scale size to small-scale model in laboratory, consisted of two layers; that is, a subbase layer and a pavement layer. The subbase layer was modified and replaced by KMUTT sand. The polymer modified asphaltic concrete and geosynthetics were used in the pavement layer.

3.2.1 KMUTT sand

Subbase layer in this study was modified and replaced by King Mongkut's University of Technology Thonburi Sand (KMUTT sand) as shown in Figure 3.4. It is originally sedimented river bed sand from Ratchaburi province, Thailand. KMUTT sand was firstly prepared by sieving the original sand to pass through sieve No.40 (0.425 mm) and to retain on sieve No.100 (0.150 mm). Subsequently, it was washed by tap water to remove dust as well as undesired materials and then dried by an oven at temperature of 140 °C for 24 hours to make it dried and eliminate any organic matter. Properties of KMUTT sand is shown in Table 3.2.

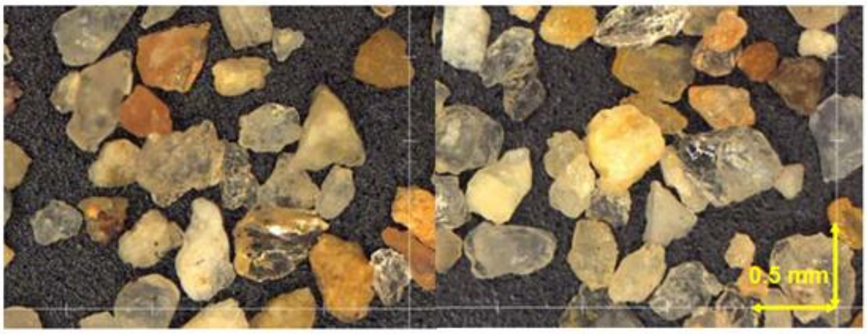

Figure 3.4 Particle photo of KMUTT sand.

Table 3.2 Properties of KMUTT sand.

Specific gravity G_s	CBR (%)	Limit void ratio		Particle distribution			Particle shape
		Max. void ratio, e_{max}	Min. void ratio, e_{min}	Mean particle size, D_{50} (mm)	Uniformity coefficient, C_u	Coefficient of Gradation, C_c	
2.64	13.49	1.06	0.71	0.285	1.879	0.946	Sub-angular

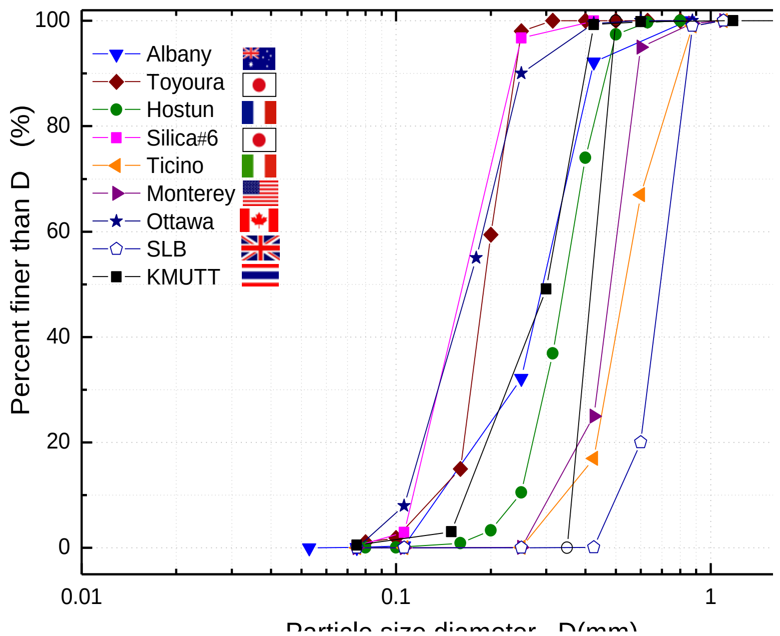

Figure 3.5 Particle distribution of standard sands and KMUTT sand

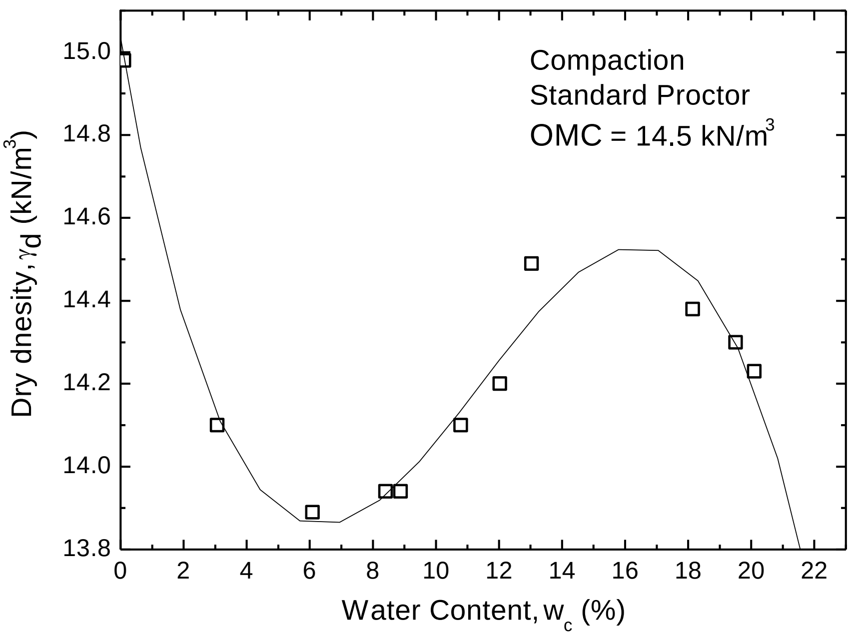

Figure 3.6 Density of KMUTT sand

3.2.2 Aggregate

An aggregate was prepared based on the Department of Highways, Thailand (DOH) Standard Test Number DOH 408/2532. The aggregate was scaled-down about 1.5 times from standard because the thickness of pavement was decreased from full-scale pavement, as shown in Figure 3.7. The aggregate was firstly prepared by sieving. This aggregate was sieved to remove particles larger than 12.50 mm, as shown in Table 3.3.

The maximum particle size of aggregate is restricted by the specimen size ratio, defined as the ratio of the specimen diameter to the maximum particle size, which should be greater than six times (Head, 1982). Then, it was washed by tab water and dried by oven at the temperature of 140°C for 24 hours to make it dried.

From sieve analysis and specific gravity test, the physical properties of aggregate are as follows;

The maximum diameter (D_{max}) = 12.50 mm
The mean particle size (D_{50}) = 2.55 mm
The coefficient of curvature (U_C) = 25
The specific gravity (G_s) = 2.63

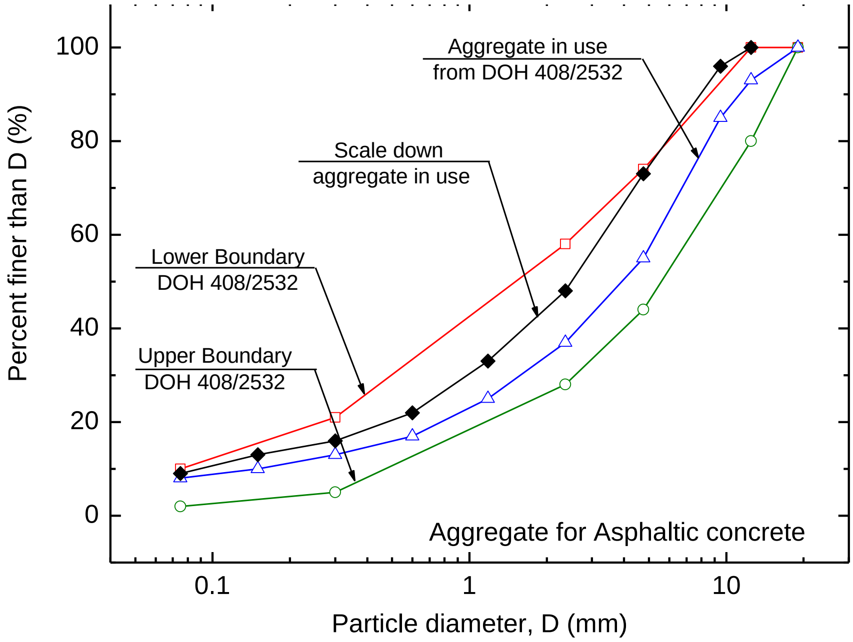

Figure 3.7 Grain size distribution curve of aggregate use for preparation of asphaltic concrete

Table 3.3 Gradation of aggregate

Sieve size (mm)	Percent passing
12.5 (1/2”)	100
9.5 (3/8”)	93
4.75 (No.4)	72
2.36 (No.8)	48
1.18 (No.16)	31
0.600 (No.30)	21
0.300 (No.50)	14
0.150 (No.100)	10
0.075 (No.200)	7

3.2.3 Polymer Modified Asphaltic Cement (PM-AC)

Polymer Modified Asphaltic Cement (PM-AC) is an improved version of Asphalt Cement produced by adding either natural polymer (such as para rubber) or synthetic polymer (such as SBS or EVA) together with an additive. A type of PM-AC, which was prepared for use in this study, is Styrene Butadiene Styrene (SBS) mix with asphalt cement 60/70 (AC-60/70). The characteristic of PM-AC is viscous, semi-solid and black. The physical properties of PM-AC are shown in Table 3.4.

Table 3.4 Properties of Polymer Modified Asphaltic Cement (PM-AC) (DH-SP. 408/2536)

Properties		PM-AC	
		Min.	**Max.**
Penetration at 25 °C (77 °F), 100 g, 5 s	0.1 mm	60	70
Softening Point, Ring and Ball	degree C	70	-
Ductility at 13 °C ,5 cm per min	cm	55	-
Torsional Recovery at 25 °C	percent	70	-
Density at 25 °C	gm/cc	1.00	1.05
Flash point (Cleveland open cup)	degree C	220	-
Solubility in Trichloroethylene	percent wt.	99	-
Test on Residue from Thin Film Oven Test			
Weight Loss	percent wt.	-	0.5
Retained Penetration at 25 °C	percent	70	
Ductility of residue at 25 °C (77 °F), 5 cm per min	cm	40	

3.2.4 Asphaltic cement

Asphaltic cement of type AC-60/70 was used to prepare test specimens in this study. The characteristic of asphaltic concrete is viscous, semi-solid and black. The physical properties of asphaltic cement are shown below.

Table 3.5 Properties of asphaltic cement

Properties	Penetration Grade 60-70	
	Min.	Max.
Penetration at 25 °C (77 °F), 100 g, 5 s 0.1 mm	60	70
Flash point (Cleveland open cup) degree C (F)	232 (450)	- -
Ductility at 25 °C (77 °F), 5 cm per min cm	100	-
Solubility in Trichloroethylene percent	99.0	-
Thin-film oven test, 3.2 mm., 163 °C (325 °F), 5 hour		
Loss on heating percent	-	0.8
Penetration of residue percent of original	54	-
Ductility of residue at 25 °C (77 °F), 5 cm per min cm	50	-
Loss on heating, 163 °C (325 °F), 5 hour percent	-	0.8

3.2.5 Geosynthetics

Two types of geosynthetics were used in this study; geogrid and geotextile. Geogrid (PGG 50) was engineered materials suitable for subgrade stabilization and base reinforcement applications. It was made from fiber grass and coated with bituminous material. On the other hand, geotextile (PGM-G 50/50) is a mechanically bonded non-woven PP continuous filament. It was made from polypropylene, UV stabilized**,** and Glass filaments**.** PGM-G grade was especially developed for the repair of asphalt road surfaces. Therefore, it was characterized by a high bitumen storage capacity. The characteristic and properties of both geosynthetics are shown in Figure 3.7, Table 3.6, and 3.8.

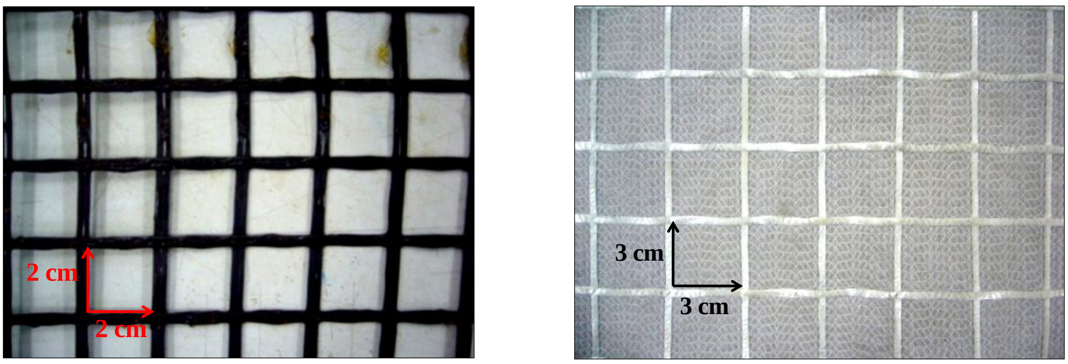

(a) (b)

Figure 3.8 Characteristic of: (a) geogrid (PGG 50); and (b) geotextile (PGM-G 50/50)

Table 3.6 Properties of Geogrid (PGG 50)

Property	Test Standard	Unit	Value
Tensile strength (warp)	ISO 10319	kg/m	50
Tensile elongation (warp)	ISO 10319	%	4
Tensile strength (weft)	ISO 10319	kg/m	50
Tensile elongation (weft)	ISO 10319	%	4
Aperture size	-	mm	20 x 20
Mass per unit area (g/m^2)	ISO 9864, ASTM D5261	g/m^2	335

Table 3.7 Properties of Geotextile (PGM-G 50/50)

Property	Test Standard	Unit	Value
Asphalt retention	Texas DOT Item 3099, ASTM D6140-97	kg/m^2	1.1
Tensile strength (md/cd)	-	kN/m	50 / 50
Elongation at break	ISO 3341	%	3
Strength at 2 % strain	-	kN/m	34 / 34
Mesh width of the glass filaments	-	mm	40 x 40
Mass per unit area	EN ISO 9864	g/m^2	300

3.2.6 Rubber membrane

Natural latex sheets were used for lubrication on the front and back windows of the model, as show in Figure 3.9. This can be done by smearing a thin layer of HIVAC-G grease on the surface of the acrylic plates. Then, layers of 0.3 mm-thick natural latex sheets were placed on the smeared grease. Therefore, the natural latex sheet can deform easily following the motions of sand particles of which their interface with the natural latex sheet is firm. In addition, by means of markers printed on the natural latex sheet, observation of motion can be recorded by photograph. Subsequent, strain fields can be determined by a photogrammetric analysis.

Figure 3.9 Rubber membrane

3.3 Apparatus

3.3.1 Container

A container was used to construct small-scale model of the pavement structures for testing in laboratory as shown in Figure 3.10. The design of this container was performed in from Japan (Hirakawa, 2003). The dimension of container is 180 cm in width, 80 cm in height, and 40 cm in deep (the out-of-plane direction). It consists of metal frame, 4 rollers and 2 acyclic plates. The container can be slid to a side by means of these roolers and a pair or rails. The acyclic plates, which are enclosed by the metal frame, are transparent. Deformation of pavement and subbase was the easily seen. Therefore, photogrammetric analysis was used in this study to analyze strain field.

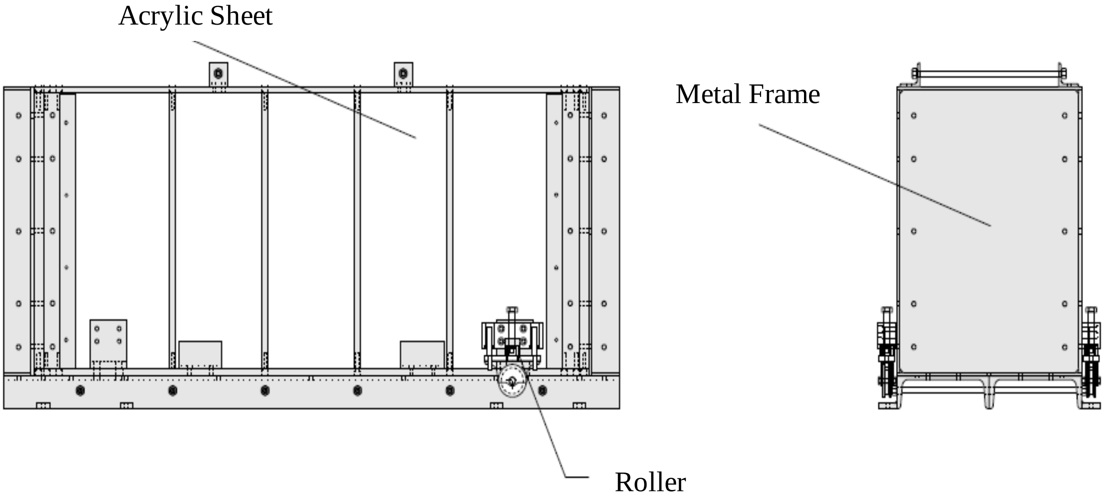

(a)

Figure 3.10 Details of the container: (a) Drawing of container and (b) Picture of container

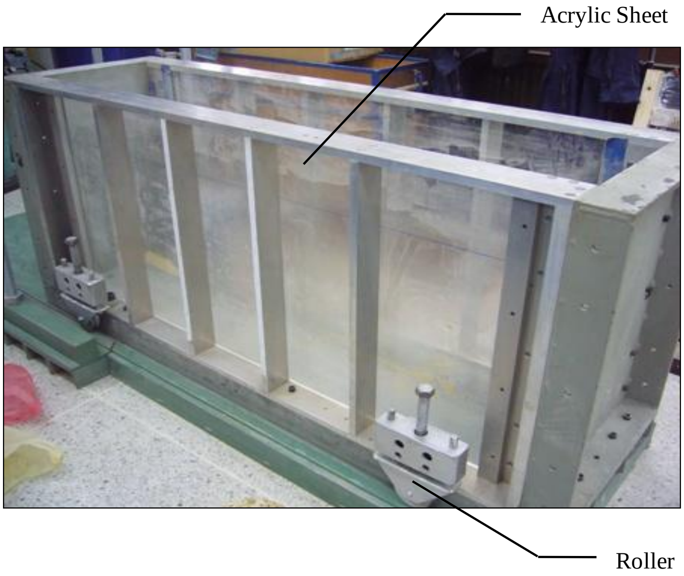

(b)

Figure 3.10 **(Cont.)** Details of the container: (a) Drawing of container and (b) Picture of container

3.3.2 Loading Frame

There are 2 main parts in loading frame; air cylinders and footing model. The first part consists of 4 air cylinders, 2 metal plates, 4 universal joints (link ball) and 4 metal bars (Figure 3.11). The air cylinders were installed on the upper metal plate and connected with link balls, metal bars and the lower metal plate. Load capacity of each cylinder is 5 kN. Thus, the maximum load, which can provide to the footing, was equal to 20 kN. Then, the lower metal plate was connected with another metal bar, axial connector, an axial load cell, linear bush and footing model in the second part. The dimensions of model footing are 6 cm in width, and 40 cm in length. All loads from air cylinders (20 kN) was transferred to the modeled footing in vertical direction. This load is a simulation of the load from wheel. The detail of loading frame is shown in Figure 3.10.

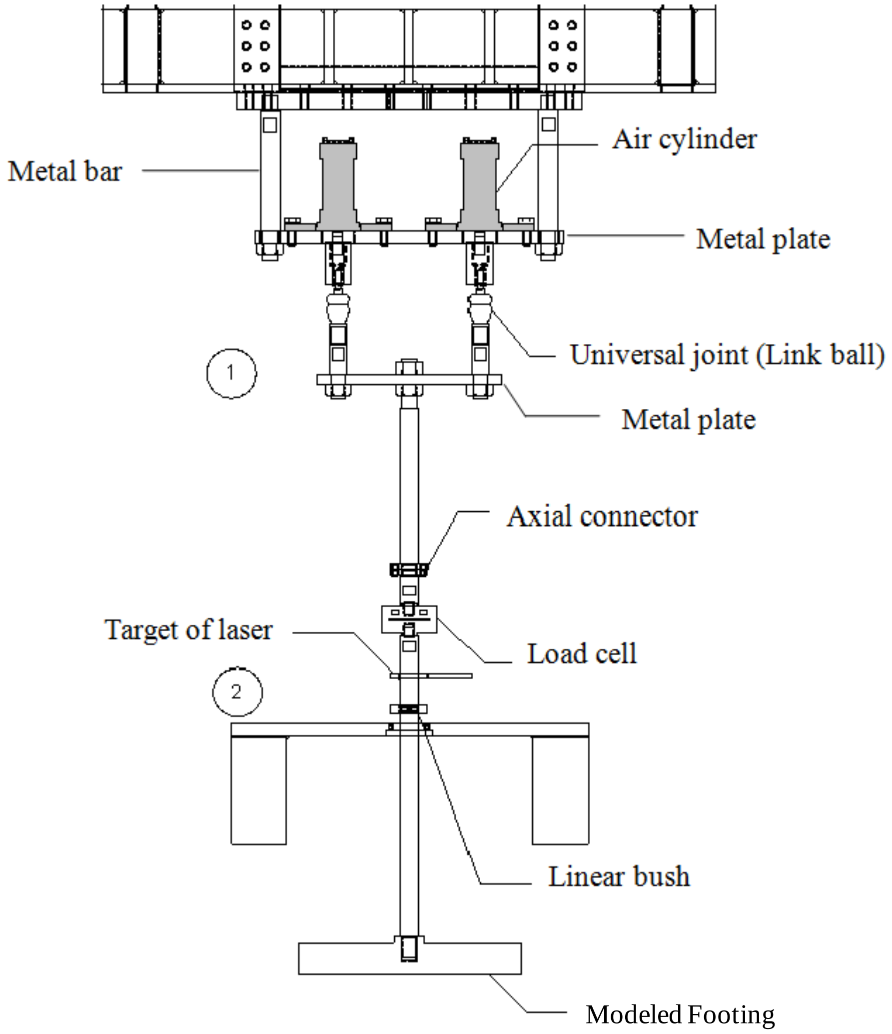

(a)

Figure 3.11 Details of loading frame: (a) Drawing of loading frame and (b) Picture of loading frame

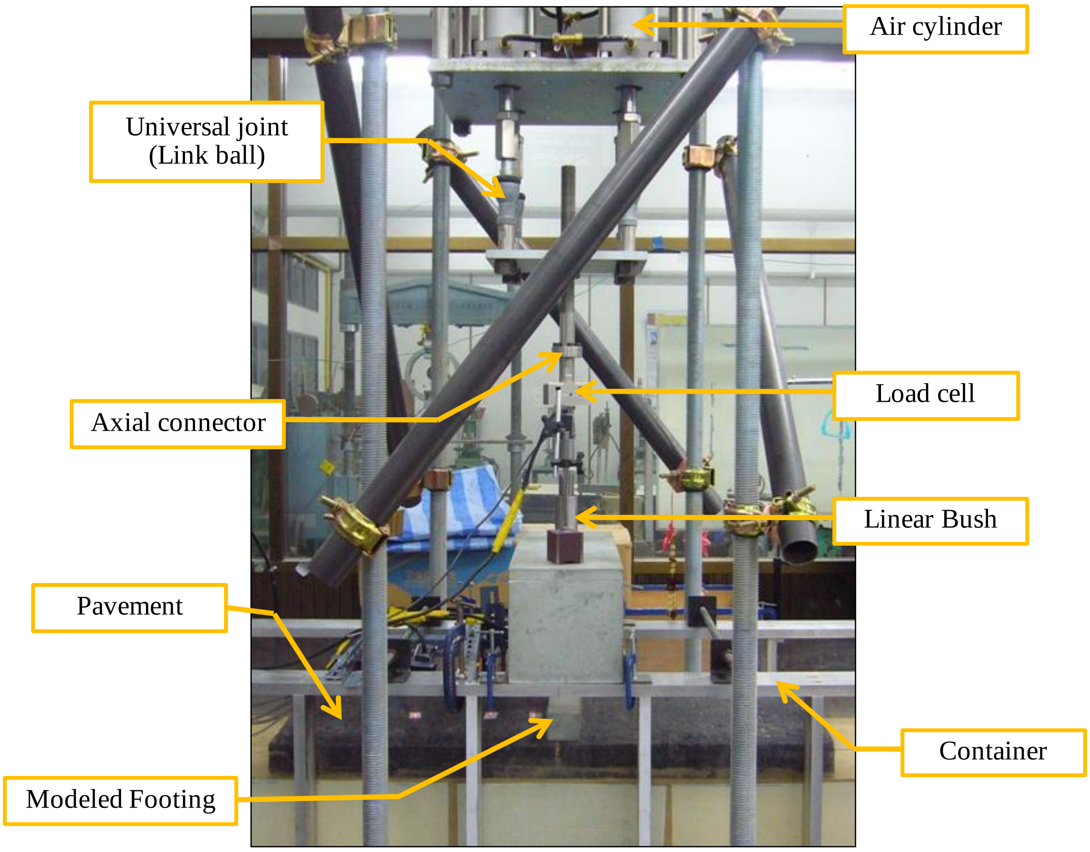

(b)

Figure 3.11 **(Cont.)** Details of loading frame: (a) Drawing of loading frame and (b) Picture of loading frame

3.3.3 Multiple Sieving Pluviation Apparatus

A multiple sieving pluviation apparatus was used to prepare subbase layer by pluviating KMUTT sand through air into the container. In this study, the multiple sieving pluviation apparatus was modified and made based on the typical pluviation manner in preparing triaxial sand specimen as shown in Figure. 3.12(a) (Miura and Toki, 1982). It consists of 5 opening sieve layers. The dimensions of the multiple sieving pluviation apparatus are 50 cm in width, 120 cm in length, and 60 cm in height, as shown in Figure 3.12(b). By this apparatus, layer of KMUTT sand was prepared uniformly and the density can be controlled successfully.

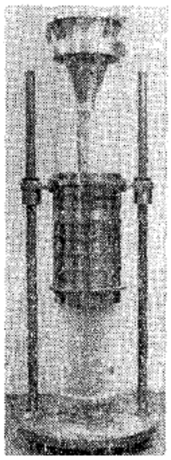

Figure 3.12(a) Typical pluviation manner in preparing triaxial specimen of sand (Miura and Toki, 1982)

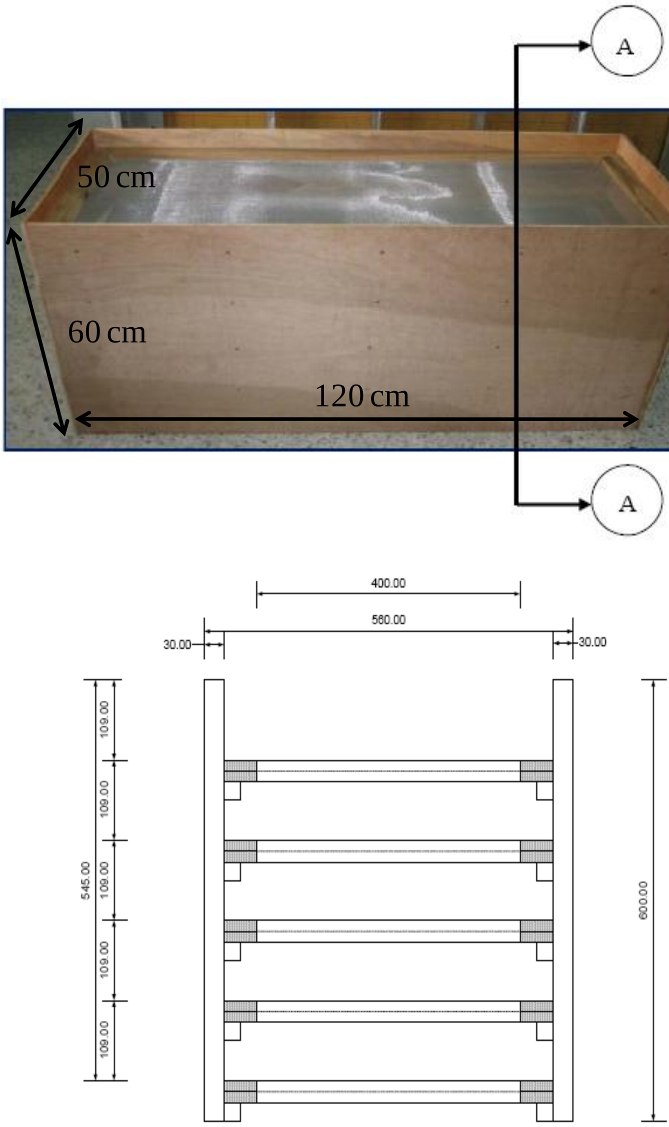

Section A-A

Figure 3.12(b) Multiple sieving pluviation apparatus for preparing subbase layer in this study

3.3.4 Mold

A Mold, used for preparation pavement, was made of steel bars and plywood. The characteristic of mold is rectangular prismatic. The inner dimensions of mold are 38.5 in wide, 103 in long and 10 cm in thick.

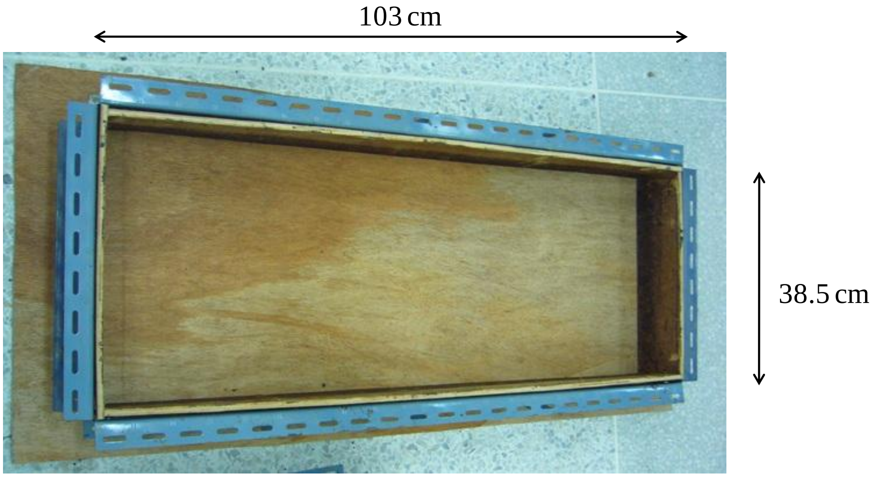

Figure 3.13 The characteristic of mould

3.4 Test Preparation

3.4.1 KMUTT sand base (Subbase)

A natural latex membrane with printed markers and other five sheets without markers were attached on the acrylic plates by HIVAC-G silicone grease (Figure 3.15). The position for attaching these sheets is shown in Figure 3.15. Then, KMUTT sand is pluviated into the container by the multiple sieving pluviation apparatus. The required height of KMUTT sand was 60 cm.

Figure 3.14 Grease

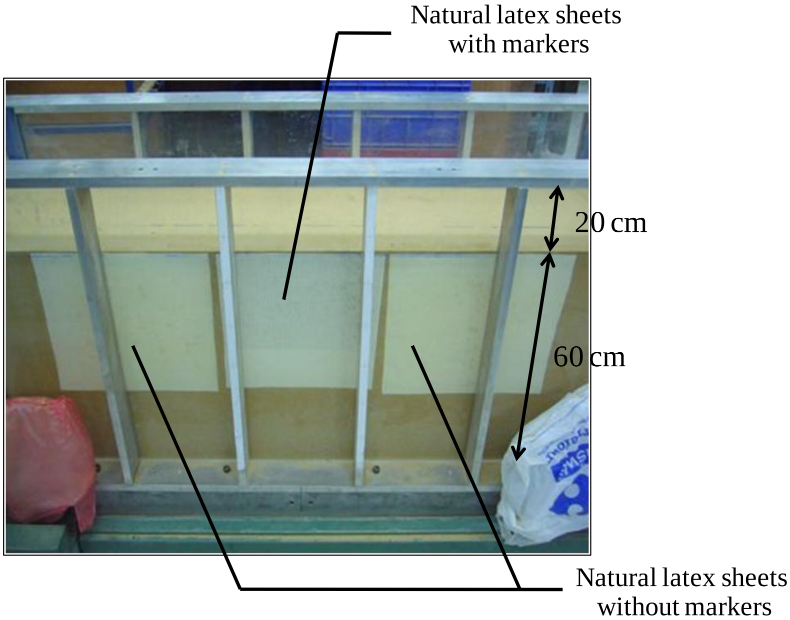

Figure 3.15 Preparation of the modeled subbase

3.4.2 Polymer Modified Asphalt (PMA)

The hot-mix method was used for mixing polymer modified asphalt cement (PM-AC) with aggregates in this study.

3.4.2.1 Heating

The PM-AC was heated by hot oil at 180 $\pm 5\,^{o}C$ about two hours for mixing new pavement. The aggregates were also heated in an oven for about two hours at temperature of 180 $\pm 5\,^{o}C$. This temperature is suitable for mixing PMA (Tipco, 2006). The asphaltic cement (AC) and aggregates were heated in an oven for about two hours at temperature of 140 $\pm 5\,^{o}C$ for mixing old pavement.

3.4.2.2 Mixing

After being heated, PM-AC or AC and aggregates, which were hot, were mixed together in a hot tray on stove. The ratio between PM-AC and aggregates was 5:100 by weight. This ratio was determined at optimum asphaltic content based on the Marshal's test results (Thaisri, 2007).

3.4.2.3 Compaction

The pavement was compacted into 4 layers by hammer. The required densities were different between new pavement and overlayed pavement. For new pavement, the required density was 2.1 g/cm^3. But, the required density for overlayed pavement was 1.8 g/cm^3 for old pavement and 2.1 g/cm^3 for new pavement, as shown in Figure 3.16. Geosynthetics was installed at the assigned positions (Figure 3.16), because it conveniently installed. Although geosynthetics was placed at upper one-third of base layer is most effective in retarding reflection cracking. (Khodaii et al., 2009 and Abu-Farsakh and Chen, 2011). Geosynthetics was installed at the bottom of pavement for new pavement and the interface between new and old pavement for overlayed pavement.

After temperature of specimen has decreased, brings it out from mold. Then, the specimen was cured for at least 16 hours before installation into the container (ASTM D6927).

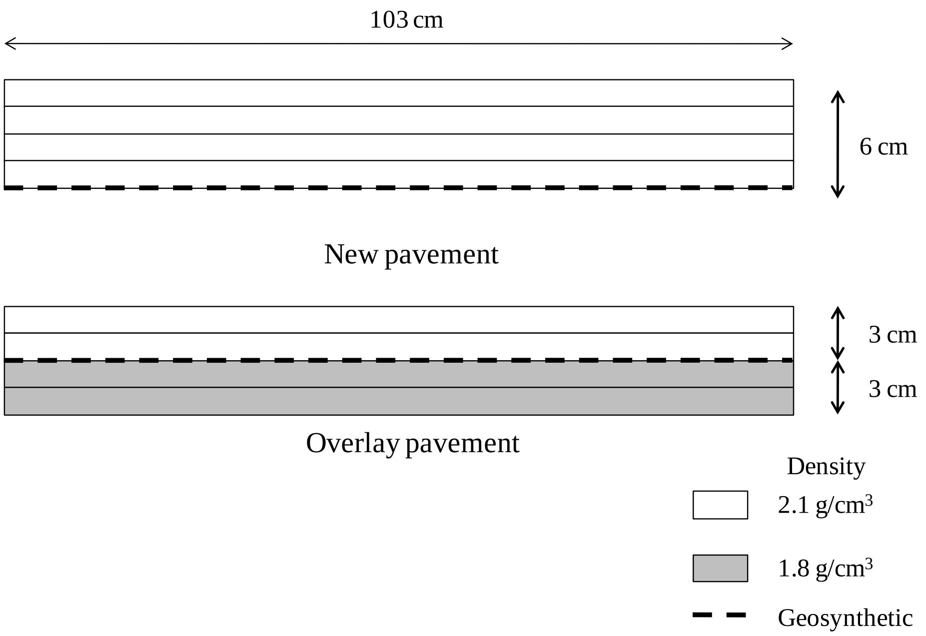

Figure 3.16 Pattern of compaction PMA

(a)

(b)

(c)

(d)

Figure 3.17 Preparations of PMA (a) Heating PM-AC, (b) Mixing PM-AC and aggregates, (c) Compaction, and (d) Compacted PMA

3.4.2.4 Installation

The PMA was checked for its density before installation into the container. Then, PMA was placed on KMUTT sand subbase, as shown in Figure 3.18. Attention must be paid to avoid bending PMA during carring.

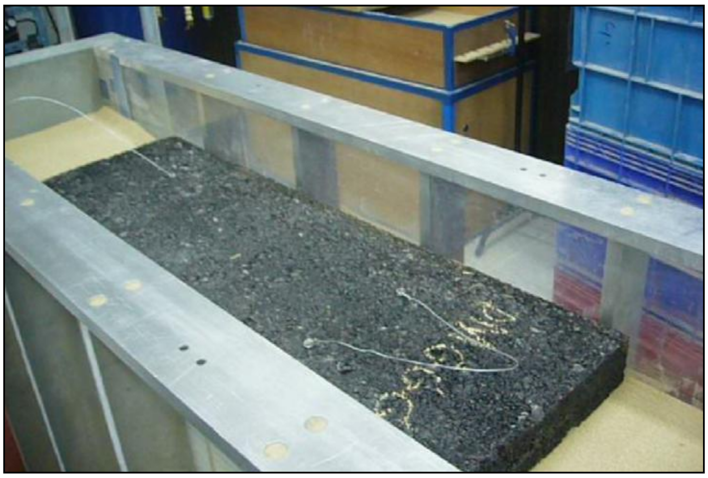

Figure 3.18 Installation PMA on KMUTT sand

3.5 Measuring devices

3.5.1 Load Cell

A load cell was used for measurement of axial load, which was applied to the modeled footing. The shape of load cell was shown in Figure 3.19(a). Four strain gages, which were manufactured by Kyowa Co. Ltd., Japan, were glued on the top of the load cell's body, as shown in Figure 3.19(b) with adhesive (Hirakawa, 2002).

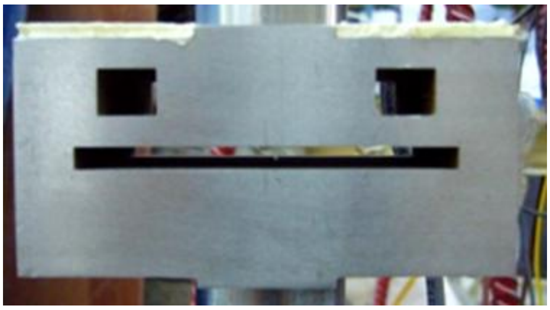

(a)

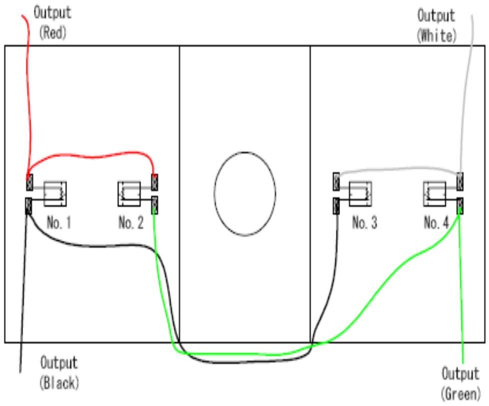

(b)

Figure 3.19 Details of load cell (a) The shape of load cell, and (b) Attachment of four strain gages on the top surface

3.5.2 Laser Displacement Sensors

The laser displacement sensors were used for the measurement of vertical displacement of the physical model of flexible pavement. There are 4 of laser sensors used in this study. One sensor was used to measure the modeled footing settlement while the other 3 sensors to measure the surface settlement of the pavement at distance of 60 mm (1D), 150 mm (2.5D) and 300 mm (5D) from the center of modeled footing respectively. D is width of footing model (6 cm).

Figure 3.20 Laser sensors

3.6 Set up of testing

After PMA was placed on subbase in container, loading frame was adjusted down for placing on PMA. Position of the modeled footing was at center of PMA. Then, laser sensors and targets were installed on the locations described above. All of measuring devices were connected with computer. Then, loading program was put in computer program. The cyclic load was used for applying load to PMA. The maximum and minimum pressure is 400 and 10 kPa and a load rate is 2,600 N/min, as shown in Figure 3.21. The load rate may change while testing, but the effect of load rate is insignificant for cyclic load (Kongsukprasert and Tatsuoka, 2007).

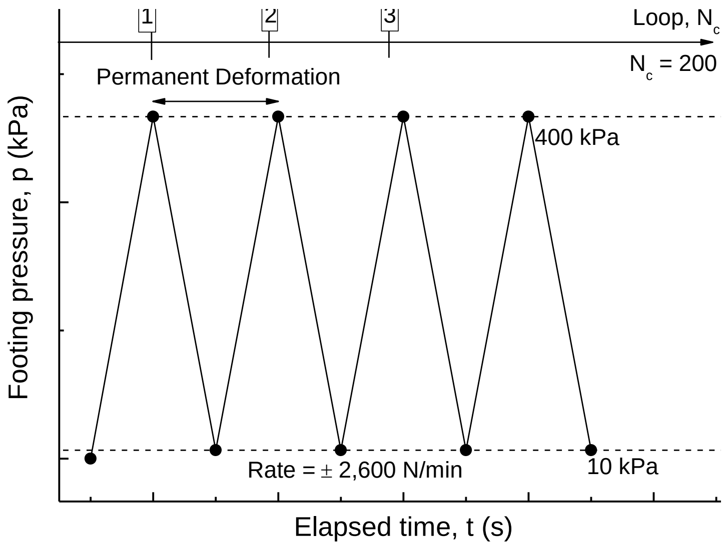

Figure 3.21 Loading program

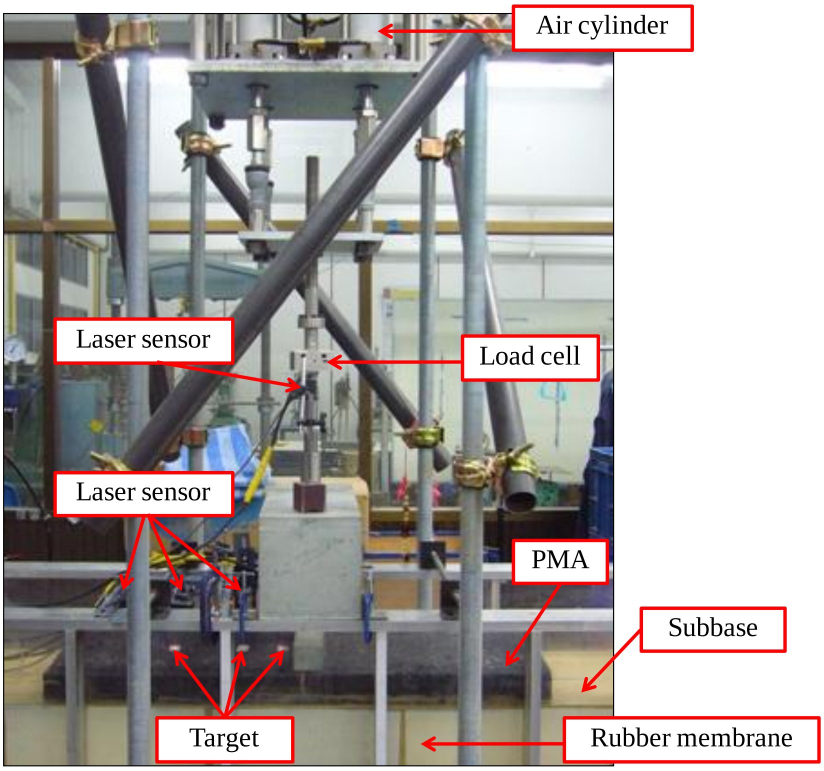

(a)

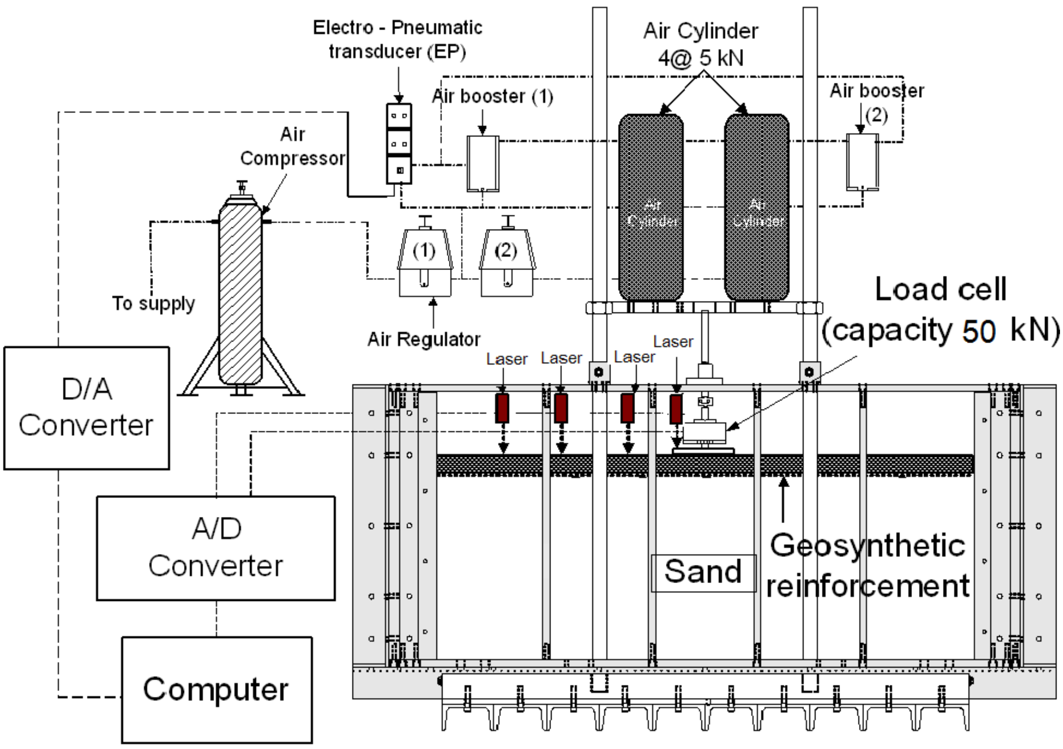

(b)

Figure 3.22 (a) picture of Apparatus A, and (b) air-circuit of Apparatus B

3.7 Test program

There were 2 cases of test program; new pavement and overlayed pavement, as shown in Table 3.8 and Figure 3.23.

Table 3.8 Test program in this study

Case	Name	Reinforced
1. New pavement	NPNO	Non-reinforced
	NPGG	Reinforced with PGG - 50
	NPGT	Reinforced with PGM - G50/50
	NPGGGT	Reinforced with PGG – 50 and PGM - G50/50
2. Overlayed pavement	DMNO	Non-reinforced
	DMGG	Reinforced with PGG - 50
	DMGT	Reinforced with PGM - G50/50
	DMGGGT	Reinforced with PGG – 50 and PGM - G50/50

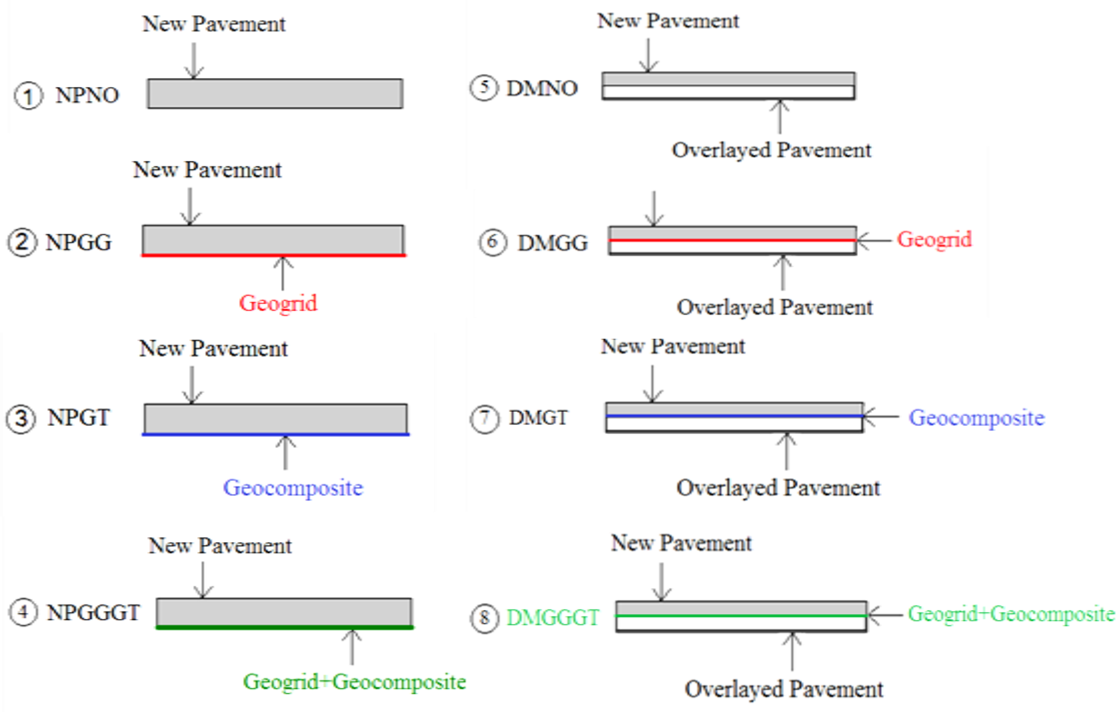

Figure 3.23 Test program in this study